EPJ Web of Conferences **291**, 03011 (2024) https://doi.org/10.1051/epjconf/202429103011
MESON 2023

Search for the Y(2175) in photoproduction at GlueX

Klaus Götzen[1] and *Frank* Nerling[1,2,3,*], on behalf of the GlueX Collaboration

[1]GSI Helmholtzzentrum für Schwerionenforschung GmbH
[2]Helmholtz Forschungsakademie Hessen für FAIR (HFHF)
[3]Goethe Universität Frankfurt am Main

Abstract. The $Y(2175)$, recently renamed to $\phi(2170)$, is one of the rare exotic candidates connected to strangeonium as compared to the heavier charmonium-like and bottomonium-like exotic states. Originally observed in initial state radiation events by the BaBar experiment in 2006, it is suggested to be a strange partner state of the charmonium-like exotic vector state $Y(4230)$ that was one of the first of the so-called XYZ states reported in the charmonium mass region. The $Y(2175)$ has been seen in various experiments and decay channels,but it has not yet been searched for in a photo-production experiment. In this talk we report on a measurement of the production cross section of the reaction $\gamma + p \rightarrow \phi\pi^+\pi^- + p$ based on data recorded by the GlueX experiment in order to search for $Y(2175) \rightarrow \phi\pi^+\pi^-$.

1 Introduction

Given the numerous candidates of charmonium-like exotic XYZ states reported since the beginning of the millennium, such as the $X(3872)$, the $Y(4230)$ or the $Z_c(3900)$, the topic of exotic bound states of the strong interaction has gained new momentum. For a recent review see e.g. [1]. Whereas the $X(3872)$, recently renamed to $\chi_{c1}(3872)$ according to the new naming scheme by the PDG, was the first of the XYZ states discovered in 2003 by the Belle experiment, the $Z_c(3900)^{\pm}$ first reported by BESIII is a manifestly exotic state, most presumably a four-quark state. The supernumerary vector state $Y(4230)$ discovered by the BaBar experiment in events with initial state radiation (ISR) is, among other interpretations, suggested to be a molecular four quark state or a charmonium hybrid state.

Analogous exotic candidates have been reported in the bottomonium sector as well. Although less conclusive, there has also significant progress been achieved in the light quark sector, where promising light hybrid meson candidates, such as the $\pi_1(1600)$ and the $\pi_1(1400)$, had been reported and studied for decades. Based on the largest data sets accumulated with a 190 GeV/c pion beam on a liquid hydrogen (proton) target with the COMPASS experiment, both $P-$wave structures observed in that data, the $\pi_1(1600) \rightarrow \eta'\pi$ and $\pi_1(1400) \rightarrow \eta\pi$, have been published from a partial-wave analysis of the 2008 COMPASS data [2]. Recently this COMPASS result has been re-analysed in a coupled-channel analysis by JPAC, in which both, the $\pi_1(1600)$ and the $\pi_1(1400)$ can be described by a single exotic π_1 resonant pole with $J^{PC} = 1^{-+}$ [3].

*Corresponding author, e-mail: F.Nerling@gsi.de

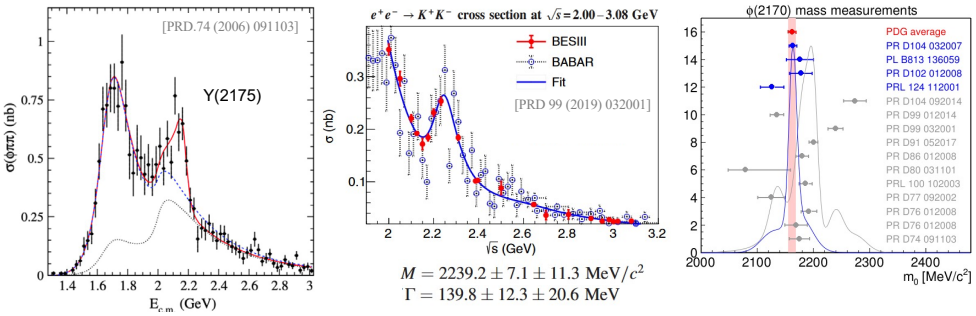

Figure 1. *Left:* Discovery plot by BaBar [4]. *Centre:* A measurement by BESIII [5]. *Right:* Compilation of individual measurements (not provided by PDG), summarised are all measurements listed by the PDG, and indicated by blue colour are those used by the PDG for their average values

The $Y(2175)$, in the meantime renamed to the $\phi(2170)$ by the PDG, was first reported by Babar in ISR [4] (Fig. 1, left) and it has meanwhile been confirmed by different experiments and decay channels. This state is proposed to be the strange partner state of the $Y(4230)$. The measured resonance parameters such as the mass vary significantly for the different measurements (Fig. 1, right). A recent measurement by BESIII [5] for instance reports a mass of about 2.24 GeV/c^2 (Fig. 1, centre), which is about 80 MeV/c^2 larger than the current PDG average value of 2162 MeV/c^2 [6]. All the available experimental information of the production of this state so far is restricted to e^+e^- experiments.

Given the many exotic candidates reported since 2003 in the heavy-quark sector and the latest results in the light meson sector as well as the progress on the theoretical side, new production mechanisms have to be explored to further pin down the nature of these states.

2 The GlueX experiment at JLab

The GlueX experiment is dedicated to the study of such exotic states in photoproduction. It is operated at Jefferson Lab in the experimental Hall D (Fig. 2, left). The electron beam provided by the Continous Electron Beam Accelerator Facility (CEBAF) is converted into a linearly polarised photon beam using the coherent bremsstrahlung technique on a thin diamond radiator, and the coherent peak is at about 9 GeV, where the degree of polarisation achieved is about 40 %. The fixed-target spectrometer (Fig. 2, right) is optimised to reconstruct a wide range of charged as well as neutral final state particles. Though mainly dedicated to map out and study exotic light hybrid mesons, GlueX offers unique capabilities and allows for access to states up to the charmonium region.

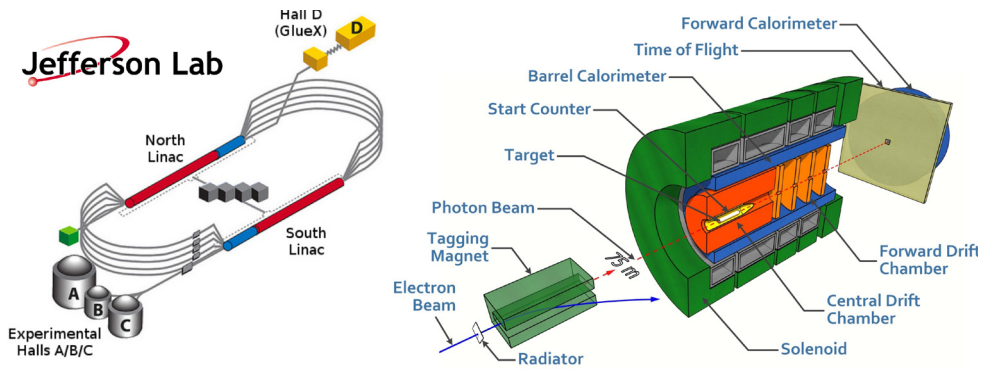

Figure 2. *Left:* Schematic of Jefferson Lab's CEBAF accelerator facility where the GlueX experiment is located in Halld-D. *Right:* The GlueX fixed-target experimental setup.

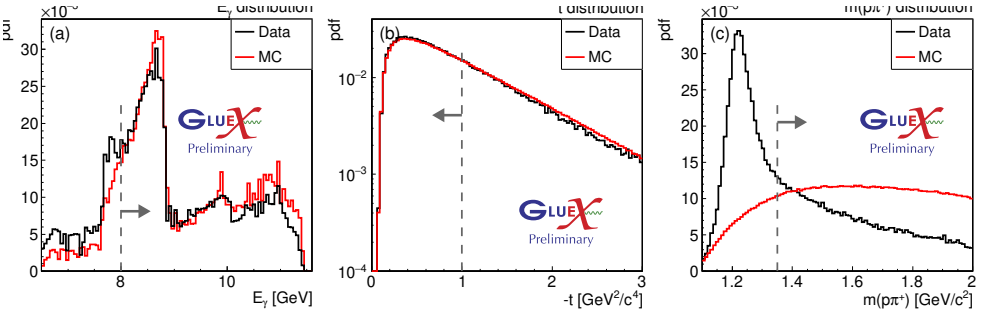

Figure 3. Event distributions for MC simulated and real data with the applied event selection cuts indicated. *Left:* Distribution of the beam photon energy E_γ (a). *Centre:* Distribution of the squared momentum transfer $-t$. *Right:* Invariant mass of the (πp) system.

The GlueX Phase-I data analysed and presented here was collected in three different periods in 2017 and 2018. The corresponding integrated luminosity for $E_\gamma > 8\,\text{GeV}$ is $304\,\text{pb}^{-1}$ in total, namely $53\,\text{pb}^{-1}$, $153\,\text{pb}^{-1}$, and $98\,\text{pb}^{-1}$ for the 2017, Spring 2018 and Fall 2018 data takings, respectively.

3 Analysis of $\gamma p \to \phi\pi\pi p$ photoproduction

According to a theoretical prediction, the $Y(2175)$ is expected to be produced with a 8 GeV photon beam with a cross section of about 1000 pb [7]. Instead of the $\eta\phi$ decay channel addressed in that study, we have performed a measurement of the differential cross-section measurement for the $\phi\pi\pi$ decay channel in order to benefit from larger reconstruction efficiencies for charged final state particles as well as an expected larger branching fraction.

3.1 Selection of exclusive $\phi\pi\pi$ events

The event selection consist of basically three parts. After applying merely loose particle identification (PID) based on dE/dx and time-of-flight information, the $\gamma K^+K^-\pi^+\pi^- p$ event candidates are formed. We apply a 4C kinematic fit of the $K^+K^-\pi^+\pi^- p$ to the γp system together with a vertex fit. Then we apply the following five event selection criteria. We restrict ourselves to the photon beam energies $E_\gamma > 8$ GeV (Fig. 3, left), and the squared momentum transfer $-t < 1\ \text{GeV}^2/c^4$ to reduce baryonic contributions (Fig. 3, centre). A veto cut to suppress Δ^{++} is applied by requiring $m(\pi^+ p) > 1.35\,\text{GeV}/c^2$ (Fig. 3, right). The exclusivity of the event sample we ensure by a missing mass cut of $|MM^2| < 50\,\text{MeV}/c^2$ and a cut of $\chi^2_{\text{4C+vertex}} < 70$. The latter two cuts are optimised using the figure of merit of the ϕ signal in data. Finally we determine the ϕ yield as a function of the $\phi\pi^+\pi^-$ mass and thus the yield of $\phi\pi^+\pi^-$ events as needed for the differential cross-section measurement. The cut on the momentum transfer $-t$ was applied also on the MC generator level, and the cross section results presented are thus to be understood as "fiducial" measurements restricted to just this $-t$ range.

3.2 Measurement of the differential photoproduction cross section

The reconstruction efficiencies as well as the ϕ yield are determined for 40 equidistant mass slices along the $\phi\pi^+\pi^-$ mass between $1.4\,\text{GeV}c^2$ and $3.2\,\text{GeV}c^2$. The efficiencies are obtained by dividing the reconstructed by the the generated MC events for each mass bin, resulting in values of about 3 % to 7 % depending on the given data set (Fig. 4, left). A clear ϕ signal band

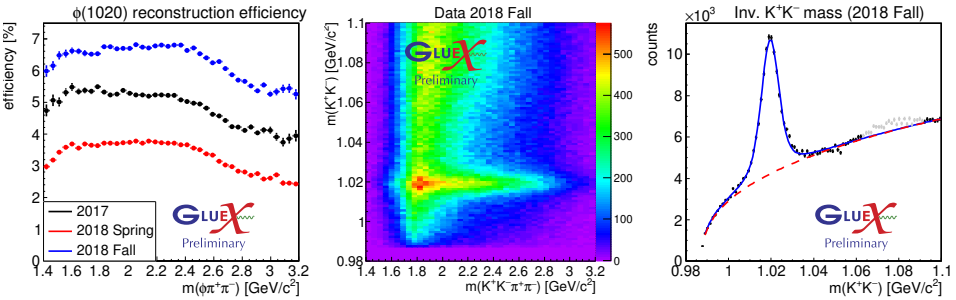

Figure 4. *Left:* Mass-dependent reconstruction efficiencies as determined for the different data sets (a). *Centre:* Invariant mass distribution $m(K^+K^-)$ versus $m(K^+K^-\pi^+\pi^-)$ exemplary shown for the "2018 Fall" data set (b). *Right:* Accumulated ϕ peak in the "2018 Fall" data together with the ϕ and background model as applied with fixed parameters for the slice-wise fits to extract the ϕ yields from data.

is visible in the $m(K^+K^-)$ vs. $m(K^+K^-\pi^+\pi^-)$ invariant mass together with the background present in the data, as shown for the 2018 Fall data (Fig. 4, centre). We extract the $m(\phi\pi^+\pi^-)$ event yield by fitting the ϕ signal in these bins of $m(\phi\pi^+\pi^-)$. The ϕ signal in data is shown for the 2018 Fall data together with the signal fit function, which is a Voigtian plus an empirical phase space function to describe the background (Fig. 4, right). The resonance parameters of the ϕ and the resolutions are thus obtained from the data and then fixed for the slice-wise fits to extract the ϕ yields.

Using the the mass-dependent reconstruction efficiencies (Fig. 4, left), we obtain from the slice-wise extracted ϕ yields (Fig. 5, left) the differential mass-dependent $\phi\pi^+\pi^-$ cross section for each of the three data sets (Fig. 5, centre) according to the following formula with the measured photon flux F and the target thickness d_{target}:

$$\frac{\mathrm{d}\sigma}{\mathrm{d}m} = \frac{N_\phi(m_i)}{\epsilon(m_i)\cdot F\cdot d_{\text{target}}\cdot \mathcal{B}(\phi(1020)\to K^+K^-)}\,. \tag{1}$$

We combine the cross-section measurements for each of the three data sets by applying the weighted average method [6], and obtain the resultant final mass-dependent differential cross-section measurement (Fig. 5, right). Here, the systematic errors are included in quadratic sum with the statistical ones (represented by the inner error bars), leading to the total (outer) errors bars. To estimate the systematic uncertainties, the sources as listed in Tab. 1 have been considered. The corresponding different cuts and values are accordingly varied, and for each variation the ϕ yield extraction and thus the complete cross-section measurement is repeated. To stay conservative, we take the difference in the resulting cross section after each variation as compared to the default values and finally add all differences quadratically as the total systematic uncertainty.

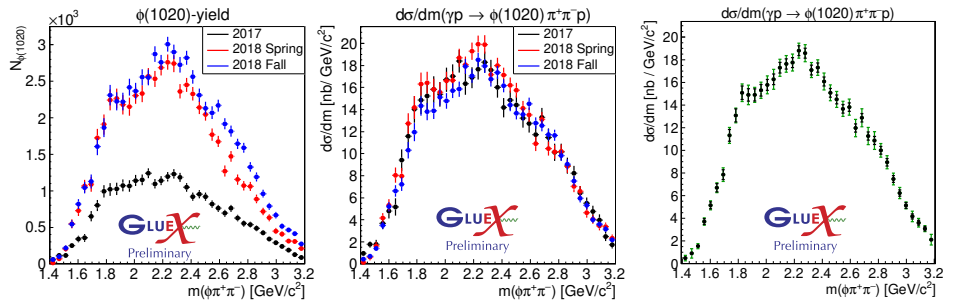

Figure 5. *Left:* Extracted mass-dependent ϕ yields. *Centre:* Differential cross section for the different data sets (b). *Right:* Final combined differential cross section, including systematics; the outer error bars represent the total and the inner ones the statistical uncertainties.

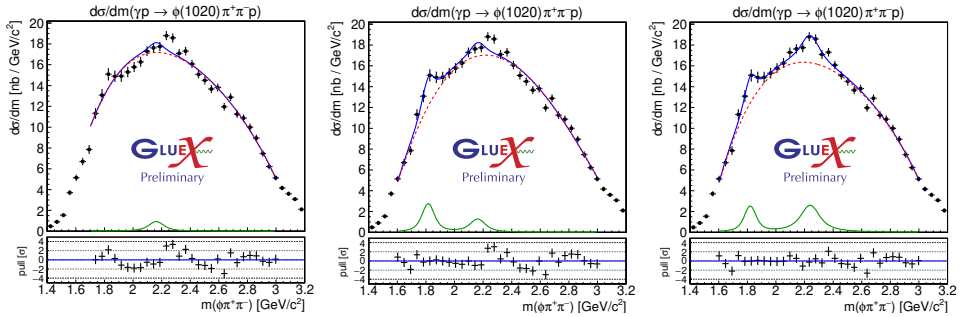

Figure 6. Search for the $Y(2175)$ and further resonances in the measured differential photoproduction cross section. *Left:* Fit model A_1 with one resonance $Y(2175)$ assuming the average resonance parameters quoted by the PDG . *Centre:* Fit model A_2 with two resonances, the $Y(2175)$ assuming the average resonance parameters quoted by the PDG and a possible second structure at a mass of about 1.8 GeV/c^2. *Right:* Fit model B_2 with two resonances, the $Y(2175)$ assuming the resonance parameters from the BESIII measurement [5] and a possible second structure at a mass of about 1.8 GeV/c^2.

3.3 Search for $Y(2175)$ and further resonances

One of the main motivations for the cross-section measurement presented (Fig. 5, right) is to address the $Y(2175)$ for the first time in photoproduction. As it can be seen (Fig. 5, right), we find a signal peak at around the $Y(2175)$ mass. We try to fit a signal shape for the $Y(2175)$ in $d\sigma/dm$ in form of a Voigtian function, using two different resonance parameters of mass and decay width together with a 4th order Chebychev polynomial to describe the background. We take into account the mass resolution as obtained from the fits to the reconstrcuted MC simulated data.

Additional systematic uncertainties are to be taken into account for this search, namely the $m(\phi\pi\pi)$ fit range and the fit model itself, which are the resonance parameters and the background description. We vary the parameters of width and mass within $\pm 1\sigma$ of the quoted errors and the degree of the Chebychev polynomial for the background description, and we then repeat the fits subsequently. We take the (larger) difference as systematic uncertainty (to stay most conservative).

The fit model A_1 contains just one state described by a Breit-Wigner shape, the $Y(2175)$, using the fixed averaged values for mass and width quoted by the PDG [6]: $m_{\phi(2170)} = 2162\pm7$ MeV/c^2 and $\Gamma_{\phi(2170)} = 100^{+31}_{-21}$ MeV. The fit model B_1 contains a different state, namely a $Y(2239)$, using the values of mass and width as reported by the BESIII measurement mentioned above [5]: $m_{Y(2239)} = 2239.2\pm13.4$ MeV/c^2 and $\Gamma_{Y(2239)} = 139.8\pm24.0$ MeV. Moreover, we try also both fit models extended by an additional second state at lower mass (A_2, B_2).

Three out of the four different fit results are displayed in Fig. 6. Using fit model A_1 (Fig. 6, left), already by eye one sees that the data is not well described, which is also reflected in the fit quality ($\chi^2/n = 2.78$). Adding a second possible structure at about 1.8 GeV/c^2, i.e. applying fit model A_2 (Fig.6, left) slightly improves the description of the data ($\chi^2/n = 2.74$),

Table 1. Sources of systematic uncertainties considered for the cross-section measurement.

Source	$\delta_{\text{sys,avg}}$ [%]	Source	$\delta_{\text{sys,avg}}$ [%]
$\phi(1020)$ branching ratio	1.0	χ^2 cut	0.9
MM^2 cut	0.4	Accidentals	0.5
K^+K^- binning	0.7	$\Delta(1232)^{++}$ veto	2.8
$\phi(1020)$ fit model data	0.8	$\phi(1020)$ fit model MC	0.7
$\phi(1020)$ fit range	1.6	$\phi(1020)$ veto range MC	0.5
$\phi(1020)$ integral range	0.1	$\phi(1020)$ param. interpolation	0.5
		Total systematic uncertainty	4.7

Table 2. Search for the $Y(2175)$: Measured production cross sections σ [pb], upper limits at the 90 % confidence level UL [pb] and significances without (Z_{stats}) and with (Z_{tot}) systematic uncertainties.

Fit model	Cross Section σ [pb]	UL [pb]	Z_{stats}	Z_{tot}
One resonance-fit (A_1), $Y(2175)$ fixed	$174 \pm 69 \pm 218$	499	2.1	1.6
Two resonance-fit (A_2), $Y(2175)$ fixed	$232 \pm 68 \pm 91$	379	1.8	1.5
One resonance-fit (B_1), $Y(2239)$ fixed	$641 \pm 82 \pm 181$	896	6.0	5.7
Two resonance-fit (B_2), $Y(2239)$ fixed	$232 \pm 68 \pm 91$	826	5.1	4.7

however, it does not improve the description of the structure at about $2.2\,\text{GeV}/c^2$. This peak is well described when using the second set of resonance parameters [5], namely fit model B_1 for a $Y(2239)$ state ($\chi^2/n = 1.38$). When finally using fit model B_2, i.e. allowing for a second possible structure at about $1.8\,\text{GeV}/c^2$ in addition to the $Y(2239)$ the description of the data is further improved ($\chi^2/n = 1.2$).

The resultant significance of the $Y(2239)$ ranges from $Z_{\text{tot}} = 5.7\,\sigma$ ($Z_{\text{stats}} = 6.0\,\sigma$) to $Z_{\text{tot}} = 4.7\,\sigma$ ($Z_{\text{stats}} = 5.1\,\sigma$), depending on the applied fit model B_1 and B_2, respectively. While we do not find a significant signal for the $Y(2175)$ with resonance parameters quoted by the PDG, we observe for the first time a denoted $Y(2239)$ decaying to $\phi\pi^+\pi^-$ in photoproduction with a statistical significance of about 5σ with systematic uncertainties taken into account. The results of our performed search are summarised in Tab. 2.

The measured production strength of the $Y(2239)$ is found to be consistent with the theoretical prediction of 1200 pb, keeping in mind the fiducial measurement represents not the total production cross section. Moreover, we find strong evidence for a second structure at a mass of about $1.8\,\text{GeV}/c^2$. Though we do not quote fitted resonance parameters of this possible second state, we compute upper limits for such a state, resulting in $\sigma_{\text{UL(CL90)}} < 615$ pb (A_2) and $\sigma_{\text{UL(CL90)}} < 701$ pb (B_2), respectively, depending on the fit model.

4 Summary

We have provided a first measurement of the differential photoproduction cross section $\mathrm{d}\sigma/\mathrm{d}m$ for the reaction $\gamma p \to \phi\pi^+\pi^- p$ with the GlueX experiment. Based on this measured cross section, the $Y(2175)$, which is a candidate for the strange-quark partner of the $Y(4230)$, has been studied for the first time in photoproduction.

We do not find evidence ($Z_{\text{tot}} < 3$) for the $Y(2175)$ when using the PDG average values as (fixed) resonance parameters. Using alternative parameters as measured by BESIII, we observe a significant signal between $Z_{\text{tot}} = 5.7\sigma$ and $Z_{\text{tot}} = 4.7\sigma$, depending on the fit model applied. The measured signal strength of the $Y(2239)$ is found consistent with theoretical predictions for photoproduction of the $Y(2175)$. We also find evidence for a second structure at a mass of about $1.8\,\text{GeV}/c^2$. We provide upper limits for such a second state that compute to $\sigma_{\text{UL(CL90)}} < 615$ pb and $\sigma_{\text{UL(CL90)}} < 701$ pb, depending on the fit model applied.

References

[1] N. Brambilla *et al.*, Physics Reports 873 (2020) 1.
[2] C. Adolph *et al.* (COMPASS Collab.), Phys. Lett. B 740 (2015) 303.
[3] A. Rodas *et al.* (JPAC Collab.), Phys. Rev. Lett. 122 (2019) 042992.
[4] B. Aubert *et al.* (BaBar Collab.), Phys. Rev. D 74 (2006) 091103.
[5] M. Ablikim *et al.* (BaBar Collab.), Phys. Rev. D 99 (2019) 032001.
[6] R.L. Workman *et al.* (Particle Data Group), Prog. Theor. Exp. Phys. 8 (2022) 083C01.
[7] C.-G. Zhao *et al.*, Phys. Rev. D 99 (2019) 114014.